Energy Conversion and Management: X 27 (2025) 101148

Contents lists available at ScienceDirect

Energy Conversion and Management: X

journal homepage: www.sciencedirect.com/journal/energy-conversion-and-management-x

Designing the conceptual scheme of a pilot-industrial plant for desalination of coal, oil and gas-fields produced water by gas hydrate method

Mykhailo Pedchenko [a], Ivan Zezekalo [a], Larysa Pedchenko [a], Dmytro Yelatontsev [b,*], Anatolii Mukhachev [b], Volodymyr Shevchenko [b], Ihor Luts [b]

[a] National University "Yuri Kondratyuk Poltava Polytechnic", Pershotravneva Avenue 24, Poltava, Poltava Oblast, Ukraine
[b] M.S. Poliakov Institute of Geotechnical Mechanics of the National Academy of Sciences of Ukraine, 2-a Simferopolska St., Dnipro, Dnipropetrovsk Oblast, Ukraine

ARTICLE INFO

Keywords:
Gaseous hydrate
Pilot
Jet dynamics
Phase separation

ABSTRACT

The growing scarcity of fresh water on the planet is driving intensified research to improve desalination technologies for unlimited seawater and underground reservoir water resources. In addition, the process of extracting hydrocarbon minerals is accompanied by the forced extraction of associated reservoir waters. For the most part, these waters have a high level of mineralization. However, based on the capabilities of existing technologies, the effective desalination of such water is technically impossible or economically unfeasible. In contrast, the promising desalination technology based on gas hydrates is not burdened by these drawbacks. However, for widespread implementation, improvements and adaptations of technological operations to industrial application conditions are required. Based on the results of this study, a conceptual scheme for a plant for the desalination of produced water from coal, oil, and gas fields is proposed. The proposed scheme is unique because it uses a free-jet apparatus as the main element of the reactor unit. The advantages of jet technology ensure the efficient implementation of the following operations: mixing of the reactor contents, gas injection into the liquid, removal of heat of hydrate formation from the reaction zone, feeding the process with water, and removal of the produced gas hydrate from the reactor to the separation unit. In addition, to simplify the design of the equipment and increase its reliability, it is proposed to implement the process under thermobaric conditions close to equilibrium at a gas hydrate concentration in the mixture that does not exceed 15 wt%. % to prevent complications associated with the solid phase of the gas hydrate. The possibility of a one-stage gas hydrate desalination process without additional washing of the gas hydrate mass and a 79.4 % reduction in the level of water mineralization, on average, was demonstrated.

1. Introduction

The limitation of freshwater resources forces humanity to develop technologies for desalinating mineralized water and invest huge amounts of money in the development of seawater desalination. Traditional desalination methods are classified into thermal and membrane methods [1,2]. The most common thermal methods are multi-stage flash distillation (MSF), multi-effect distillation (MED), and steam compression evaporation [2].

The most common membrane methods are forward osmosis (FO) and reverse osmosis (RO) [1,3,4], which have drawbacks. For example, distillation is a popular method, but it is quite energy-intensive because it requires a large amount of energy to evaporate water [5,6], and the reverse osmosis method requires significant investment and maintenance [7,8]. In addition, membrane processes cannot treat heavily contaminated water because of fouling problems with membranes [9]. In addition, the membranes used in RO are sensitive to impurities, pH, algae, bacteria, and other contaminants [10,11]. The typical water recovery in RO is less than 55 % [5]. In addition, seawater recovery by single-stage RO is usually limited to 40 % because of membrane fouling [12]. Simultaneously, the level of total dissolved solids (TDS) that can be treated by RO membranes is usually 10–60 g/L [13,14].

All desalination processes involve the separation of mineralized water into two streams: one with a low salt concentration and the other with a high salt content [15]. Depending on the target product, the technology can be considered as desalination (the product is fresh

* Corresponding author at: M.S. Poliakov Institute of Geotechnical Mechanics of the National Academy of Sciences of Ukraine, 2-a Simferopolska St., Dnipro, Dnipropetrovsk Oblast, Ukraine.
E-mail address: iambenadar@proton.me (D. Yelatontsev).

https://doi.org/10.1016/j.ecmx.2025.101148
Received 27 January 2025; Received in revised form 9 July 2025; Accepted 9 July 2025
Available online 9 July 2025

water) or concentration (the product is a concentrate that is not part of the hydrate). In this case, both fresh water and concentrate can have commercial value. However, brines may also contain valuable resources such as magnesium sulfate, calcium carbonate, and lithium, which cannot be extracted by reverse osmosis [16].

Simultaneously, the coal, oil, and gas industries produce a huge amount of mineralized produced water. The chemical composition of produced water varies widely and depends mainly on the characteristics of the reservoir geology. Simultaneously, they are highly mineralized and contaminated with a significant amount of various impurities. Several technologies based on gas hydrates are currently available [17]. One such technology is gas hydrate-based desalination. This technology is based on the production of gas hydrates, which are crystalline solids consisting of water molecules (hosts) and hydrate-forming gases (guests) [18]. Gas hydrate-based desalination offers significant advantages, as gas molecules do not contaminate the liquid and are easily separated from the resulting fresh water. When gas hydrates dissociate, only gas and purified water are produced, without any other impurities [19–21].

Desalination based on gas hydrates is considered an alternative method [17,22]. This is due to the fact that ions and salts dissolved in liquids practically do not penetrate into gas hydrate crystals [23]. Desalination using gas hydrates consists of three stages: formation of hydrate crystals in mineralized water, separation of crystals from the residual concentrated solution, and melting of hydrate crystals [24].

In [25], 79.5–84.3 % of the dissolved mineral components were removed by a 3-stage hydrate process. This study showed that desalination hydrate formation can be applied to produce water with an initial total dissolved solids (TDS) content of up to 160 g/L. Thus, the most significant advantage of gas hydrate-based water treatment is that solutions with extremely high mineralization can be treated [13].

However, all desalination processes for separating salts from water require significant amounts of energy. Therefore, minimizing the cost of desalination processes is an important technological challenge [26].

In 1997, Yu. F. Makogon showed that gas hydrate desalination technology can be cheaper than thermal and membrane methods [17] because the formation of hydrates requires less severe thermodynamic conditions ($T < 20$ °C and $P > 30$ bar) than other phase transition methods. Therefore, gas hydrate-based technology is potentially less energy-intensive than MSF and RO [27]. However, in the absence of currently implemented projects, only an approximate assessment of its technical and economic indicators can be provided.

Simultaneously, a comparison of the characteristics of existing desalination plants of all types, for example, those given in [28,29] (Table 1), shows a significant (sometimes several times) range of their main characteristics. The fact that they have been operating for a long time indicates, at a minimum, their profitability.

A distinctive feature of gas hydrate-based technologies is the need to conduct the process under high pressure and low temperature. For highly mineralized water, such as formation water, and methane-based gas mixtures, this means a pressure of over 5 MPa and a temperature below 263 K [17], which requires the use of appropriate equipment. Simultaneously, the maximum energy consumption of the technology is associated with the cooling of mineralized water and the utilization of heat from the exothermic process of hydrate formation. The enthalpy of formation/dissociation of natural gas hydrates is in the range of 520–540 kJ/kg [30].

However, similar to other desalination technologies, the use of efficient heat exchange equipment allows up to 80 % of the energy to be recovered. Simultaneously, one of the advantages of this technology is the relatively narrow range of "comfortable" temperatures for the formation and dissociation of gas hydrates. This allows several regions to use low-potential energy from daily and seasonal fluctuations in ambient temperature. As for the consumption of electrical energy during the operation of the pump-compressor equipment complex of a gas hydrate-based desalination plant, there is no reason to believe that it will be higher than the consumption of most traditional technologies, that is, within 1.5–3.0 kWh/m^3 (Table 2). Therefore, gas hydrate-based desalination projects will be competitive when implemented.

One reason for the delay in implementing this technology is the difficulty in separating crystals from concentrated salt solutions and removing dissolved hydrate-forming agents from desalinated water. Theoretically, hydrates in the solid phase can be separated from the liquid and gas phases. However, there are still some difficulties in the hydrate separation process under certain temperature and pressure conditions [30]. Previous studies have shown that the desalination effect is not satisfactory without the effective separation of the resulting hydrates and concentrated brine [25,31]. It is important to remove residual water from the hydrate mass in a simple and rapid manner. Therefore, many studies have been devoted to the development of methods and apparatus for separating hydrates from concentrated residues [25,30–33].

In [6], a stirred bed reactor was used to remove salts from model-associated waters (salinity of 9 wt%), with a desalination efficiency of 90 %. Previous studies [22] demonstrated a continuous production unit for CO_2 hydrate granules with a desalination efficiency of 75 %. Studies [34,35] presented a ring bed reactor based on the characteristics of water migration caused by propane hydrate. In one study [36], an apparatus with a movable plunger that could divide the reactor into two chambers for hydrate formation and separation was presented. In [31], an apparatus was designed for the continuous production and extraction of granular CO_2 hydrate from a reactor using a squeezing device in the form of a perforated double cylinder covered with a metal mesh.

The available data on the kinetics of hydrate formation indicate low process rates and a low degree of water-to-hydrate conversion. This significantly hinders the practical application of gas hydrate technology

Table 1
Current state-of-art of desalination techniques development [28,29].

Technology	Average capacity (10^3 m^3/day)	Recovery ratio	Energy consumption Electrical (kWh/m^3)	Thermal (kJ/kg)	Water cost ($/m^3)
Multi-effect distillation	0.6–30	0.25	1.5–2.5	230–390	0.52–1.50
Thermal vapor compression	10–35	0.25	1.5–2.5	145–390	0.87–0.95
Multi-stage flash	50–70	0.22	4–6	190–390	0.56–1.75
Mechanical vapor compression	0.1–3.0	–	6–12	–	2.0–2.6
Seawater reverse osmosis	1–320	0.42	3–6	–	0.45–1.72
Brackish water reverse osmosis	≤98	0.65	1.5–2.5	–	0.26–1.33
Electrodialysis	≤145	0.90	2.64–5.50	–	0.60–1.05

Table 2
Analysis of the rate of gas entry into the gas hydrate depending on the method of contacting the phases in the reactor.

Agitation mode	The volume of fluid in the reactor (L)	Pressure in the reactor (MPa)	Temperature (K)	Gas intake rate (L/L per min)	Reference
Mechanical	0.3	5.6	273	0.2	[42]
Mechanical	0.3	5.8	277	0.1	[43]
Mechanical	1.0	5.5	279	1.3	[44]
Mechanical	5.6	5.4	277	1.8	[45]
Mechanical	9.6	7.1	283	2.0	[46]
Liquid stream	3.7	3.0	278	4.8	Present study

[37].

Under static conditions of hydrate formation (without mixing the reactor contents), after the appearance of crystallization centers, active hydrate growth occurs on the free water–gas surface. Water was covered with a continuous hydrate film. The hydrate formation process was significantly slowed down. Its intensification requires the continuous destruction of the hydrate film to renew the water–gas contact. For this purpose, the reactor contents were stirred.

For the efficient production of gas hydrates in reactors, water–gas interfacial contact can be realized by bubbling gas into a liquid, spraying water in a gas atmosphere, or a combination of these injection methods. In the case of gas atomization in the water–gas contact zone, hydrate formation occurs according to the following mechanism [38]:

1) gas hydrate germs are formed at the interfragment boundary;
2) a gas hydrate crust (up to 0.04 mm thick) forms on the surface of the droplet;
3) the hydrate crust gradually thickens to 0.24 mm, and water comes into contact with the gas through the capillaries present in the hydrate. The rate of hydrate formation decreased significantly.

Because water is a relatively incompressible compound, the gas pressure from the outside cannot break the hydrate crust. Consequently, a significant portion of the water is trapped in the droplets, making it difficult to separate or convert to hydrate. However, in the case of gas bubbling into water, a gas hydrate crust forms on the surface of the bubbles [39]. When the pressure outside the bubble increases, the "egg effect" is observed, in which the crust collapses inward, after which hydrate formation occurs around the crust fragments. Consequently, when water is bubbled with hydrate, significantly fewer gas bubbles are captured, thereby improving the quality of the target product. Much of the research has focused on the kinetics of gas hydrate formation and dissociation [39,40].

According to the analysis of these studies, their formation in laboratory reactors is relatively slow, taking several hours to several days. Simultaneously, the development of technologies based on gas hydrates that are acceptable for industrial implementation requires significant intensification of their production. In addition, the water–gas contact area is one of the determining parameters of the rate (productivity) of gas hydrate production. However, because hydrate formation is an exothermic process, the realization of a continuous and high-performance industrial process requires efficient heat removal, as heat removal from the reaction zone is one of the key parameters of this process.

Thus, although gas hydrate desalination technology can potentially have a number of advantages over conventional methods and has a sufficiently deep theoretical justification, there are currently no operating pilot plants for its implementation. Therefore, the purpose of this

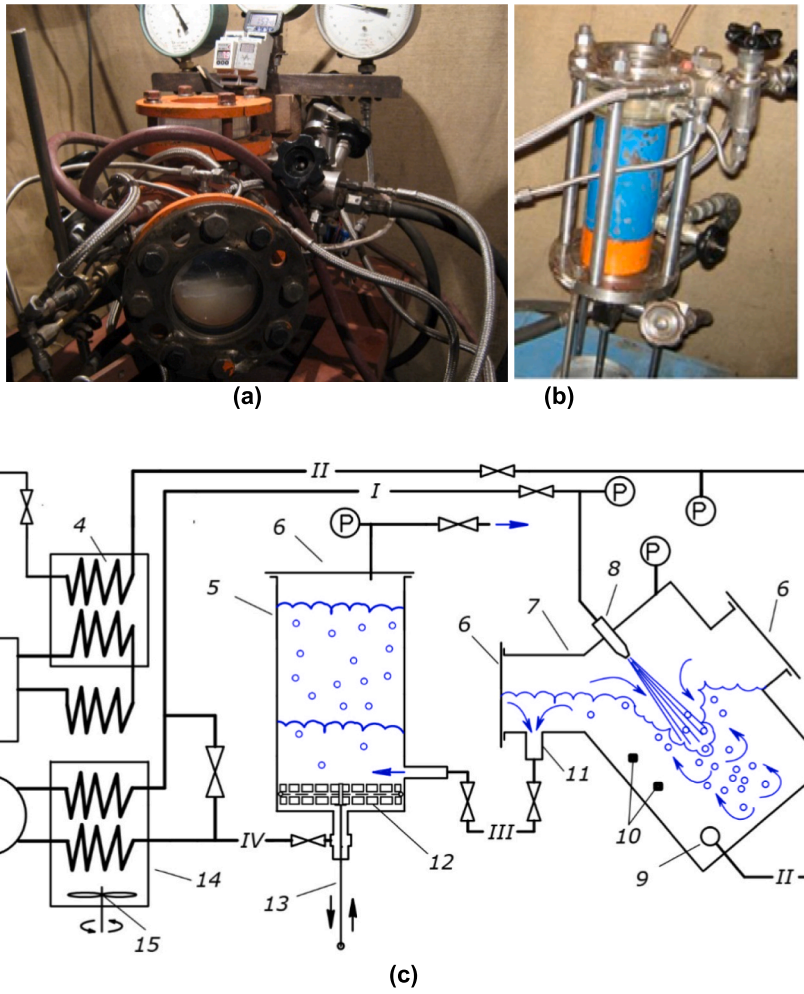

Fig. 1. Laboratory setup for studying the processes of formation and separation of gas hydrates: reactor unit (a); separator (b); schematic diagram (c): 1 – pump; 2 – refrigeration unit; 3 – gas source; 4, 14 – heat exchanger; 5 – separator; 6 – transparent window; 7 – reactor; 8 – jetting apparatus; 9 – gas bubbling device; 10 – LEDs; 11 – water–gas hydrate mixture outlet; 12 – piston with filter element; 13 – hydraulic press rod; 15 – stirrer; I – water; II – gas; III – water–gas hydrate mixture; IV – water–gas hydrate mixture depleted of gas hydrate.

study was to substantiate the basic principles and design solutions of the technological chain of production and separation of gas hydrates from formation waters of oil, gas, and coal fields to produce desalinated water and salt concentrate.

2. Materials and methods

Experimental studies were performed using the laboratory setup shown in Fig. 1.

The main purpose of the laboratory setup in this configuration was to study the fundamental possibilities and parameters of the process of continuous production and separation of gas hydrates. Gas hydrate was formed in reactor 7 as a result of mixing its contents with a water jet from jet apparatus 8. The water–gas hydrate mixture (stream III) was discharged from the reactor through connection 11 to separator 5. The main part of the free water is separated because of the pressure difference between the volume of the separator and outlet line IV, which is created during the operation of pump 1. Water filtration occurs through a filter element mounted on the piston 12. In addition, the hydrate mass can be compacted by moving piston 12 through rod 13 using a hydraulic press (not shown in the diagram). The volume of reactor 7 was 5.4 L, that of the separator was 5 – 1.4 L, and that of heat exchanger 14 with the pipeline was 1.1 L.

Coal mine methane was used as the hydrate-forming gas with the following composition (%): CH_4 = 91.8, C_2H_6 = 4.1, C_3H_8 = 1.8 and CO_2 = 2.3. Produced water with a total salinity of 183 g/L was used to demonstrate the fundamental possibility of desalinating highly mineralized fluids from coal mines, as well as oil and/or gas fields. The composition of the studied water samples was as follows (g/L): Ca^{2+} = 7.21, Mg^{2+} = 1.95, $Na^{+} + K^{+}$ = 53.1, HCO_3^- = 0.58, SO_4^{2-} = 16.5 and Cl^- = 96.7. The water sample density was 1.107 g/cm^3, pH was 5.94, and TDS was 6.71.

The temperature in the thermal chamber was maintained at 277 K, and the temperature in the reactor was maintained at 260 K (above the freezing point of the initial concentration of the solution). The gas pressure in the reactor was maintained at 6.5 MPa (above the hydrate equilibrium pressure of the components of this system). First, 5.2 L of produced water was fed into the reactor and saturated with a hydrate-forming gas. To do this, the contents of reactor 7 were first evacuated, then blown through a bubbling device 9 for 2–3 min with mine methane, the pressure was raised to 7–8 MPa and maintained for 30 min at a temperature of approximately 293 K. The procedure was repeated three to four times. Subsequently, the jet apparatus 8 was put into operation. During circulation, the mine water filled separator 5, heat exchanger 14, and the pipeline. Subsequently, approximately 2.7 L of liquid remained in the reactor. The fill level and process in the reactor were monitored using window 6.

To ensure that no supersaturated solution was formed in reactor 7 and that no salt crystals were carried over into separator 5, together with the gas hydrate, the depth of its concentration was limited by selecting 10–12 % of water in the hydrate composition (i.e., no more than 0.6 L of the volume of the sample under study). Approximately, this selection corresponded to the volume of separator 5 1.4 L (Fig. 1c) after maximum filling with hydrate, considering its porosity before the pressing stage. The volume of the separator was preliminarily selected by changing the cylindrical inserts.

The level of filling of the separator with the solid phase was controlled using a transparent window 6. After filling separator 7, the liquid captured from the gas hydrate was squeezed out by piston 12 using a hydraulic system 13 (Fig. 1c). To remove the sample, the gas pressure in the separator was reduced to atmospheric pressure, and the upper flange with window 6 was dismantled. After melting the sample, the total mineralization of water was determined.

To study the features of the separation of the formed gas hydrate in detail, experiments were conducted in a transparent cylindrical reactor with a moving piston (Fig. 2).

A filter mesh with a diameter of approximately 0.1 mm was mounted on the piston. When the piston moved, the liquid phase was mechanically squeezed out, and the hydrate mass was compressed. A similar piston was used in separator 5 of the laboratory setup to study the processes of formation and separation of gas hydrates (Fig. 1, element 12).

When determining the rate of hydrate formation when used as a device to create contact between the phases of the jet apparatus and a free-falling water jet, the dependence of the gas flow rate from the cylinder at a constant pressure (3 MPa) in reactor 1 (Fig. 1) on the liquid pressure in the nozzle section was observed. To initiate the gas hydrate formation process, the gas supply valve to the reactor was opened, and pump 17 was simultaneously turned on. The water supply to the nozzle of the jet apparatus was adjusted under pressure according to the repetition in the range of 3.5–7.0 MPa (the difference between the jet pressure and the pressure in the reactor was 0.5–4.0 MPa). The temperature in the reactor stabilized at 278.2–278.8 K after 40–70 s from the beginning of its circulation.

Based on the characteristics of the jet apparatus and the experimental values of the fluid pressure, the jet velocity was determined using the following equation:

$$Q_{water} = \mu_H \omega_H \sqrt{2gp/\rho g} = \sqrt{2p/\rho}\,\mu_H \omega_H \quad (1)$$

where Q_{water} is the fluid flow rate through the nozzle (m3/s), μ_H is the nozzle flow coefficient, ω_H is the cross-sectional area of the nozzle (m^2), P is the pressure (Pa), ρ is the density of the fluid (kg/m^3), and g is the acceleration of free fall (m/s^2).

$$\nu_{\text{p}} = Q/\omega = \sqrt{2p/\rho}\,\mu_H \quad (2)$$

where ν_{p} is the average fluid velocity at the nozzle outlet (m/s), *and* μ_H = 0.82 (for a given cylindrical nozzle).

The formula provided in [41] was used to determine the injection capacity of the free jet.

$$Q = 5,4{\cdot}10^{-6}(\rho{\cdot}d^3{\cdot}v_p^3/\sigma){\cdot}(l/d_H)^{0,75}{\cdot}(\sin\alpha)^{-0.2} \quad (3)$$

where Q is the injection capacity (m^3/s), d is the nozzle diameter (m), σ is the surface tension coefficient (N/m), l is the nozzle length (m), *and* α

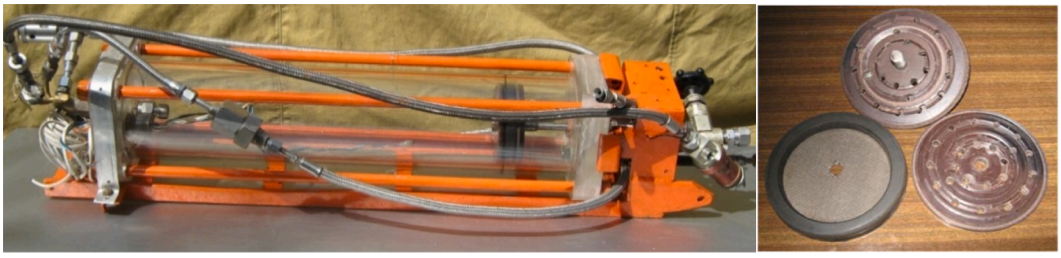

Fig. 2. Demonstration reactor with a moving piston with a filter element: a – exterior; b – piston design with a filter element.

is the angle of inclination of the injected jet to the horizontal plane.

3. Results and discussion

3.1. Study of the hydrate formation process

Hydrate formation involves dissolving gas in water under appropriate thermobaric conditions, provided that effective interfacial contact is created; hydrate structures form and grow with the release of an appropriate amount of process heat [17].

Gas-liquid contact can be created at the expense of energy:

1) Compressed gas (bubbling columns and gas lifters).
2) Mechanical mixers (self-priming stirrators).
3) Circulation pumps (injection-jet pumps).
4) Simultaneous energy input into the gas and liquid phases (when gas is forced into jet dispersers or under mechanical stirring).

To evaluate the efficiency of hydrate formation, it was assumed that gas hydrate germ formation occurred instantaneously. After the installation reaches the required process parameters, a sufficient number of crystallization germs are constantly present in the liquid phase, as their size makes it impossible to separate (the bulk of the crystallization germs). The system that describes this process consists of gas bubbles and hydrate crystals dispersed in water, and their size gradually increases. Mass transfer occurs between the three phases, and the growth of crystals is accompanied by a change in the concentration of the dissolved gas. In this case, the gradient of the concentration in the bubble-crystallization model is the driving force of the process.

Fig. 3 shows the dependence of the gas flow rate on the hydrate formation process in the reactor volume with respect to the water pressure at the nozzle section of the free-flowing jet apparatus.

The results indicate a linear relationship between the liquid pressure in the jetting apparatus and the gas consumption during hydrate formation. This dependence is described by an approximate linear function as follows:

$$y = a \cdot p + b \tag{4}$$

where y is the rate of gas entry into the gas hydrate (gas flow rate) (m^3/s), a and b are empirical coefficients, and p is the water pressure at the nozzle cut of the jetting apparatus (MPa).

The results of the calculations according to Eq. (4) in the form of the dependence of the rate of gas entry into the hydrate composition on the amount of injected gas per the entire volume of liquid in the reactor are given in Fig. 4.

The experimental dependence is described by the following equation:

$$y = 0.6829x + 0.2893 \tag{5}$$

where x is the gas injection rate (m^3/s).

The resulting coefficient of 0.6829 corresponds to the portion of gas that is part of the gas hydrate. The gas composition in the reactor, which was not included in the hydrate structure, was as follows (%): CH_4 = 99.64, C_2H_6 = 0.15, C_3H_8 = 0.03, and CO_2 = 0.18. For comparison, when mechanical stirrers are used, the coefficient a of gas incorporation into the gas hydrate is 0.44–0.56 [42].

The remaining gas, in the form of bubbles, entered the surface of the liquid. An increase in the hydrate formation rate was observed with increasing gas injection rate. Simultaneously, the intensity of release and efficiency of heat removal during hydrate formation, as determined from the heat balance, limit this process.

According to the proposed method of hydrate formation, intensive gas injection into the liquid (with a significant excess) occurs mainly because of its circulation inside the reactor between the gas cap and the water–gas hydrate mixture. At the same time, its replenishment with a new portion occurs only as a substitution after the corresponding amount of gas available in the reactor is included in the gas hydrate. Considering the significant specific consumption of liquid (water–gas hydrate mixture circulating in the system through the reactor), the average rate of gas entry into the gas hydrate composition per 1 L of liquid volume in the reactor was $0.8 \bullet 10^{-4}$ m^3/s (4.8 L/min). Table 1 shows the rate of hydrate formation depending on the phase contact method.

As the jet enters the liquid volume, gas is injected into the liquid and dispersed with the formation of the smallest bubbles of poorly water-soluble hydrocarbon gases, allowing for efficient recirculation of gas from the upper part of the reactor that has not had time to react without the use of additional compressor equipment. It is assumed that in the zone of turbulent mixing and pressure pulsations, gas bubbles undergo periodic deformation while forming a hydrate crust on their surface. This results in the continuous destruction of the hydrate crust (the "egg effect") and the formation of a new crust on the free surface [39]. The gas hydrate produced by this method will contain a minimum amount of trapped water (as part of the droplets preserved by the hydrate crust and film). This will greatly simplify the implementation of further separation of the water–gas hydrate mixture.

Thus, the requirement for intensive contact between the gas and

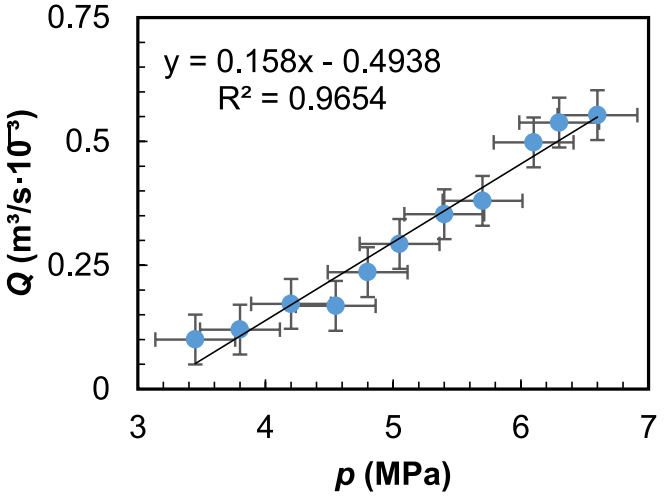

Fig. 3. Dependence of the gas flow rate on the formation of hydrate formation on the water pressure at the nozzle section of the jet apparatus with a free jet.

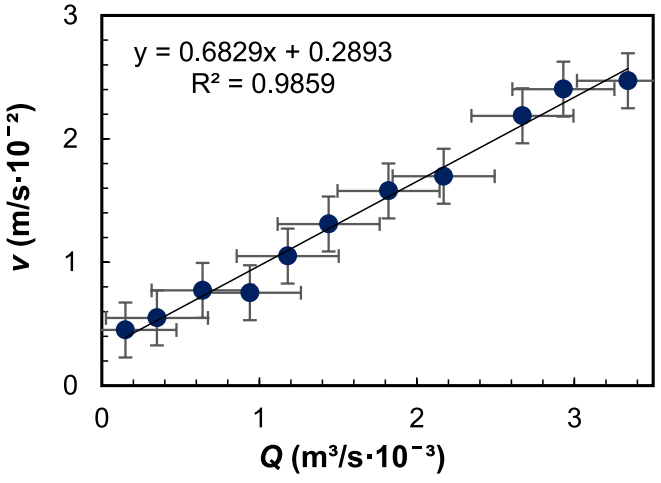

Fig. 4. The rate of entry of the gas under study into the gas hydrate composition depending on the amount of injected gas (T = 278.2 K, P = 3.0 MPa; liquid volume in the reactor – 3.7 L).

water is satisfied by reactors equipped with appropriate jetting devices. Among them, free-flow injection devices are the most promising in terms of simplicity, reliability, efficiency, and maximum consideration of gas hydrates.

3.2. Justification of process parameters and structural elements of the pilot plant

One of the problems that delay the industrial implementation of gas hydrate technologies is the threat of uncontrolled accumulation of gas hydrates on the surface of equipment and the formation of hydrate plugs. Therefore, the process of gas hydrate production may be significantly complicated up to its complete shutdown. Therefore, in addition to choosing an effective method of hydrate formation, it is equally important to organize a continuous production process by circulating material flows between the devices of a gas hydrate plant.

The formation of macrostructures (larger than 1 mm) of gas hydrate occurs as a result of the simultaneous coagulation of microcrystals with the hydrate formation process (in a continuous process simultaneously with the formation of nuclei and massive crystal growth) [17]. In the case of excess water in the hydrate formation process at temperatures above 273 K, the artificially formed gas hydrate is an amorphous porous hydrate mass formed as a result of crystal coagulation, with a significant amount of water trapped between the crystals. This mass is quite plastic, easily gives up most of its free water during separation and pressing, and is easily compacted.

Fig. 5 shows the stages of separation of the water–gas hydrate mixture and compaction of the gas hydrate in a demonstration reactor using a piston with a built-in filter element.

To ensure a continuous gas hydrate production process, it is necessary to create conditions for the constant and uninterrupted removal of the hydrate from the reactor, supply of gas and water to the reactor, and

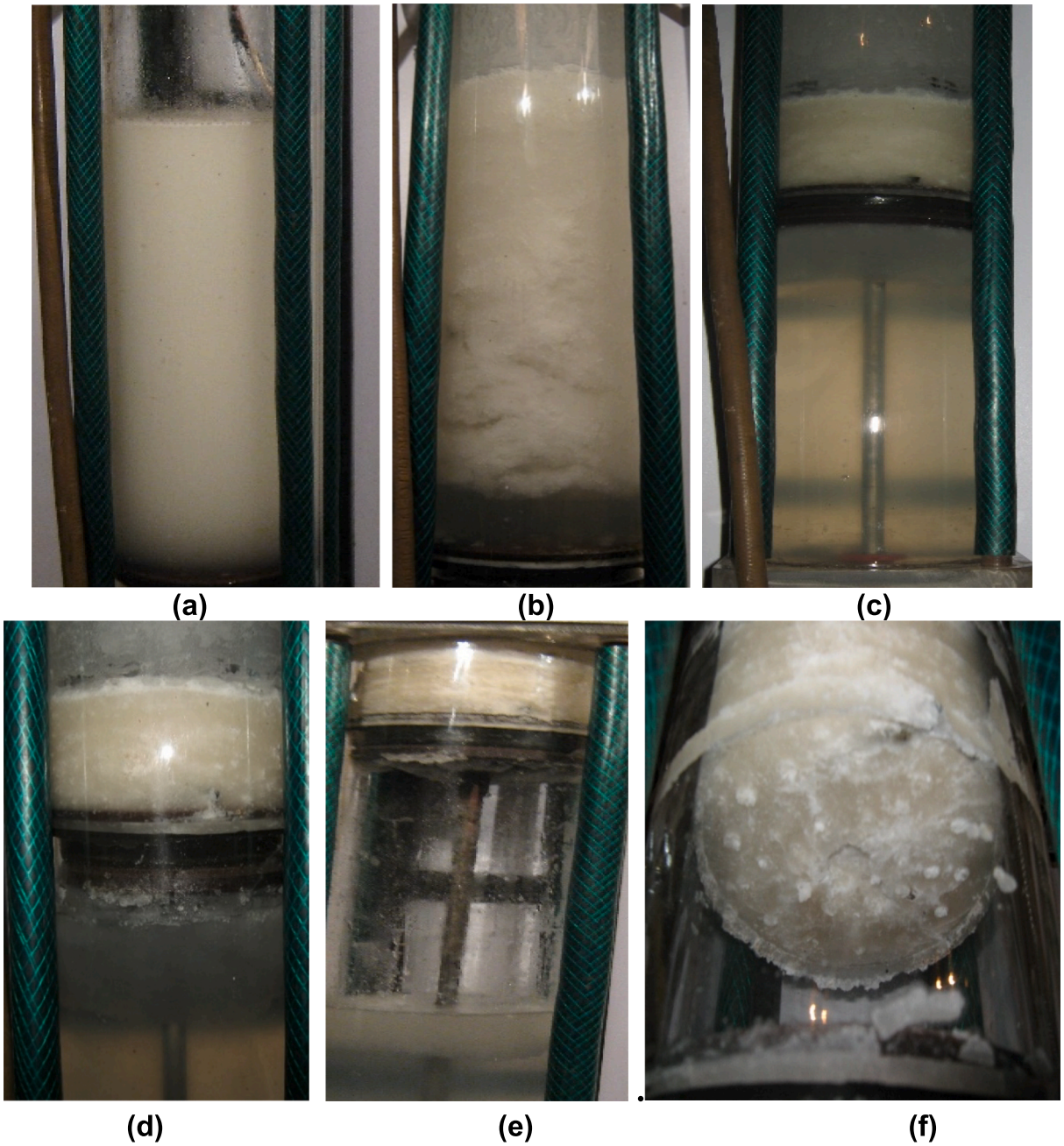

Fig. 5. Sequence of separation stages (a–f) of the water–gas hydrate mixture (removal of water through the filter element in the piston).

removal of the hydrate formation heat. The most critical part of the process is the removal of the reactor. The difficulty lies in the fact that within the thermobaric parameters of the process, the property of gas hydrate structures to grow rapidly and actively agglomerate is manifested. Simultaneously, the accumulation of gas hydrate solid phases in the process lines is undesirable, as it leads to complications associated with their blockage, formation of stagnant zones in the reactor, and deterioration of heat removal, and hence the intensity of hydrate formation.

During the separation process, it is impossible to completely separate free water from hydrate and part of the hydrate from water. Microcrystals and germs of hydrate formation penetrate the filter element in the piston and continue to grow and coagulate to sizes visible to the naked eye. Consequently, a significant number of unfiltered hydrate crystals were present in the area under the piston (Fig. 5c–e).

Consequently, a sufficient number of gas hydrate crystallization centers constantly entered the reactor with the circulation flow. This conclusion completely eliminates the need to activate the hydrate formation process by adding certain substances (e.g., surfactants) to the reactor. This makes it possible to obtain (under certain conditions) high-quality desalinated water after the dissociation of the gas hydrate.

Based on the proposed method of hydrate formation and the need for constant recirculation of water into the reactor as a raw material and working fluid for bubbling gas into a liquid volume, it would also be logical to remove the majority of the main amount of heat energy of hydrate formation from the reactor along with the water–gas hydrate mixture. Owing to the low concentration of gas hydrate in the stream, this method of heat removal will allow the refusal to use the method of cooling through the reactor walls or an integrated heat exchanger. Thus, the utilization of hydrate energy in an external heat exchanger will be as simple and efficient as possible.

Simultaneously, the rate of hydrate formation at such a pressure directly depends on the process temperature, which, in turn, depends on the rate of heat removal from the hydrate. With a high-quality phase contact and the onset of equilibrium conditions, the main parameter that determines the rate of hydrate formation, according to this method, is the method of heat utilization.

The minimum temperature of the water entering the reactor can be 273–274 K. Also, and the amount of heat from the hydrate formation process that can be neutralized by the cooled feed gas stream is negligible. In addition, the maximum process temperature is limited by the equilibrium stability parameters of gas hydrates. Therefore, the most effective way to maintain the required temperature in the reactor is to remove the heat energy of hydrate formation during the circulation of the material flow (a mixture of water and gas hydrates) through external heat exchangers. In addition, for economic and technical reasons, considering the results of the studies described below, as well as those given in [47] regarding the conditions for preventing equipment blockage by the gas hydrate mass, it is necessary to provide the process at thermobaric parameters close to equilibrium. Based on the typical composition of the associated gases and reservoir waters of coal and oil and gas fields, such conditions lie in the ranges of 281–288 K and 3.8–5.5 MPa. It has been established that to prevent the clogging of technological lines with gas hydrates, their concentration in the mixture should not exceed 15 wt%.

It is evident that when the thermobaric parameters in the reactor approach the equilibrium hydrate formation rate, the process rate decreases. Simultaneously, with an increase in the mass flow rate of the circulating flow (at a constant gas pressure), the rate of hydrate formation may increase, or the process parameters may become more stringent; that is, the temperature in the reactor will decrease if the phase contact area is limited.

Similarly, when the process parameters approach equilibrium hydrate formation, the rate of hydrate particle coagulation decreases. If we take into account the mechanical effect of stirring with a liquid jet (dispersion), we can conclude that the release of a solid hydrate phase will not occur. Thus, the coagulation of gas hydrate microparticles can be prevented by the active stirring of the reactor contents in combination with the process under relatively mild thermobaric conditions. Thus, the application of the proposed method for hydrate formation will allow for a continuous production process without complications.

As mentioned above, the most difficult element of mineralized water desalination based on gas hydrate technology is the hydrate separation stage. Based on the kinetics of the hydrate formation process in the presence of soluble salt ions, the size of the formed crystals of the solid phase of the hydrate at the stage of mass crystallization is, on average, at the level of microns. However, under certain conditions (e.g., growth, coagulation, and separation), hydrate crystals can accumulate as a continuous porous mass (e.g., hydrate plugs in industrial pipelines). However, these two states of the produced hydrate phase do not satisfy the conditions for implementing this technological process.

In this regard, experiments were conducted to demonstrate the fundamental feasibility of the process and to establish the parameters of coagulation, separation of the gas hydrate mass, and prevention of hydrate plugs. The main source of information was the visual control of the process through the reactor windows (photo and video recordings). Simultaneously, the thermobaric parameters of the process were recorded. In order for the system to reach equilibrium conditions as soon as possible (in this case, by increasing the temperature), the initial pressure was set at 2.4 MPa. The equilibrium conditions in the reactor were achieved after 95 s from the beginning of the experiment when the temperature in the reactor increased to 279.9 K.

After 8–10 s from the start of mixing, the water in the reactor became cloudy, and after 15 s, it was white. During the mixing time of 4 min, no signs of solid-phase formation were observed in the water–gas hydrate mixture. At the same time, the liquid droplets that hit the walls of the reactor and its elements, starting from the fifth minute (when the concentration of gas hydrate reached a certain level) and the mixture in the inspection window nozzle (where a stagnant zone was formed) began to form a jelly like structure (Fig. 6). After 30–90 s (depending on the repetition), obvious phase separation was observed. The same phenomenon occurred in the entire reactor volume after the stirrer was turned off.

A similar pattern was observed for the hydrate formation process in the demonstration reactor (Fig. 7). However, in our opinion, because the thermobaric conditions were more severe for this gas composition (typical coal mine methane composition) and the hydrate concentration was quite high at the time of fixation, the reactor contents after stopping the mixing were a rather unstable suspension of hydrate particles in the water, and the gas hydrate content was approximately 24 vol%. Moreover, these particles were visible to the naked eye (above the piston) and had a fairly uniform size (0.2–0.4 mm). Simultaneously, after stopping the stirring, unlike the first case, phase separation due to active coagulation occurred within 3–5 s (Fig. 6b).

In addition, a significant portion of the gas hydrate remained in the solution with a size of less than 0.1 mm. Fig. 7 shows how a translucent liquid with no visible signs of solid-phase formation passes through the filter element of the piston, which has a mesh size of $\leq$ 0.1 mm. However, in the area under the piston, 30–60 s after the cessation of stirring, clear signs of the coagulation of hydrate crystals and their gravitational separation (a layer of clear liquid on the border of the lower flange of the reactor) were recorded (Fig. 5d and 5e).

Thus, according to the results of experimental studies, when a system with gas hydrates approaches equilibrium conditions and with intensive mixing of the reactor contents, the coagulation of solid-phase particles slows down. In the future, the process in the reactor and process lines will proceed without complications (without blockage by the hydrate mass), provided that the pressure is maintained at 0.3–0.5 MPa above the equilibrium pressure at the corresponding temperature. A similar approximate range of parameters for the slow coagulation of gas hydrates for natural gas was observed previously in [48].

Thus, based on the studies performed, the following can be

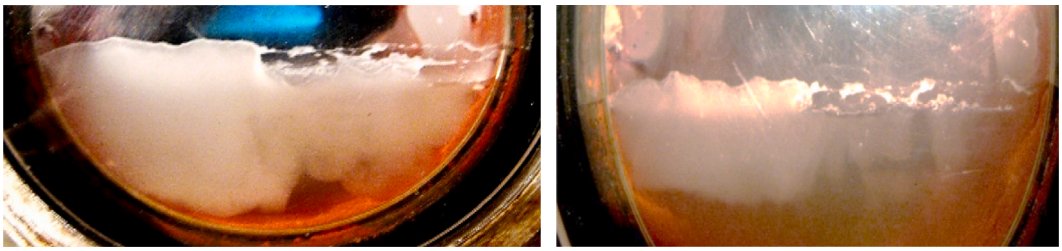

Fig. 6. Examples of the formation of a gas hydrate with a jelly like morphology under conditions close to equilibrium.

Fig. 7. The process of filtering the reactor contents through the filter element in the moving piston of the demonstration reactor.

concluded:

1) The process of hydrate formation to prevent the coagulation of gas hydrate (and, as a result, reactor plugging) should be carried out under thermobaric conditions close to equilibrium.
2) Exceeding the concentration of hydrate in the mixture above a certain critical level leads to the active release of the solid phase of gas hydrate; therefore, it is necessary to continuously remove it.
3) In the process of industrial production, the length of the line for moving the water–gas hydrate mixture from the reactor to the separator, its speed, and the thermobaric conditions created should be such that by the time the target product enters the separator, it is qualitatively coagulated.
4) By controlling the cooling rate of the circulating flow in the external heat exchangers of the plant, it is possible to control and regulate the intensity of gas hydrate formation in the reactor and its concentration in the mixture.

The separation efficiency of the formed gas hydrate mass and the level of desalination of the brine were determined. The gas hydrate mass accumulated in the separator was compressed using a moving piston to maximize liquid removal. Simultaneously, the liquid was removed through the filter element built into it. The principle of this process is illustrated in Fig. 5 (sectors c–f). Samples for the study were obtained from the main separator (Fig. 1b) at a pressure of 15 MPa. After melting the samples, the average mineralization of the water was reduced by 79.4 % (i.e. from 183 to 37.7 mg/L).

This variant of the final stage of the technological process (separation) is quite effective; however, in our opinion, its stage (accumulation–pressing–melting) is not ideal for industrial implementation and therefore requires further improvement.

Thus, the experiments have shown the fundamental possibility of organizing the process of continuous production and separation of gas hydrates in a laboratory setup (Fig. 1), the schematic diagram and design solutions of which are proposed as a prototype for an industrial installation.

The implementation of projects for the industrial implementation of the technology for desalination of produced water from oil, gas, and coal fields based on gas hydrate technology should begin with the study and justification of the following interrelated factors:

1) Based on the energy balance of technological process elements (cold production, compression, hydrate melting, hydrate solid phase separation, and regenerative heat exchange between streams), economically acceptable depth of desalination of produced water, gas concentration (e.g., coal mine methane), and brine if it is the target product.
2) Technically achievable depth of desalination of produced water, gas concentration, and/or produced water at the current level of technology.

4. Conclusions

A schematic diagram of a plant for desalinating water with high mineralization (e.g., produced water from coal, oil, and gas fields) is proposed, in which a free-jet apparatus is the main element of the reactor unit, ensuring the effective implementation of the technological process. Its use will simplify the design of the equipment but increase reliability and simultaneously ensure the following operations: mixing the contents of the reactor, injecting gas into the liquid, removing the heat of hydrate formation from the reaction zone, feeding the process with water, and removing the produced gas hydrate from the reactor to the separation unit.

To prevent the clogging of technological lines with gas hydrate deposits, it is proposed to implement the process under thermobaric conditions close to equilibrium, when the coagulation of the formed hydrate crystals in the reactor is minimal. These conditions are met by the process pressure, which is only 0.3–0.5 MPa higher than that of equilibrium hydrate formation. Also, for this purpose, it is proposed to maintain the concentration of gas hydrate in the reactor no higher than 15 wt%.

In preliminary experimental studies, it was established that it is possible to reduce the level of water mineralization by an average of 79.4 % in a one-stage gas hydrate desalination process (without additional washing of the gas hydrate mass, but with effective mechanical squeezing of the concentrate).

CRediT authorship contribution statement

Mykhailo Pedchenko: Funding acquisition, Formal analysis, Data curation, Conceptualization. **Ivan Zezekalo:** Investigation, Formal

analysis, Data curation. **Larysa Pedchenko:** Resources, Methodology, Investigation, Formal analysis, Conceptualization. **Dmytro Yelatontsev:** Writing – original draft, Visualization, Validation. **Anatolii Mukhachev:** Writing – original draft, Supervision, Conceptualization. **Volodymyr Shevchenko:** Writing – original draft, Validation, Supervision, Conceptualization. **Ihor Luts:** Writing – original draft, Formal analysis.

Declaration of competing interest

The authors declare that they have no known competing financial interests or personal relationships that could have appeared to influence the work reported in this paper.

Data availability

Data will be made available on request.

References

[1] El-Agouz SA, Abd Elbar AR, Aboghazala AM, Shahin M, Zakaria MY, Esmaeil KK, et al. Comprehensive parametric analysis, sizing, and performance evaluation of a tubular direct contact membrane desalination system driven by heat pipe-based solar collectors. Energy Convers Manag 2022;274:116437. https://doi.org/10.1016/j.enconman.2022.116437.

[2] Shalaby SM, Hammad FA, Zayed ME. Current progress in integrated solar desalination systems: prospects from coupling configurations to energy conversion and desalination processes. Process Saf Environ Prot 2023. https://doi.org/10.1016/j.psep.2023.08.058.

[3] Shalaby SM, Zayed ME, Hammad FA, Menesy AS, Elbar ARA. Recent advances in membrane distillation hybrids for energy-efficient process configurations: Technology categorization, operational parameters identification, and energy recovery strategies. Process Saf Environ Prot 2024;190:817–38. https://doi.org/10.1016/j.psep.2024.07.098.

[4] Aboelmaaref MM, Zhao J, Zayed ME, Li Y, Gu L, Askalany AA, et al. Design and dynamic numerical modeling of a hybrid reverse osmosis/adsorption-based distillation system driven by solar dish Stirling engine for enhanced performance and waste heat recovery. Process Saf Environ Prot 2023;180:324–38. https://doi.org/10.1016/j.psep.2023.10.012.

[5] Shannon MA, Bohn PW, Elimelech M, Georgiadis JG, Mariñas BJ, Mayes AM. Science and technology for water purification in the coming decades. Nature 2008;452:301–10. https://doi.org/10.1038/nature06599.

[6] Cha J-H, Seol Y. Increasing gas hydrate formation temperature for desalination of high salinity produced water with secondary guests. ACS Sustain Chem Eng 2013;1:1218–24. https://doi.org/10.1021/sc400160u.

[7] Rubina B, Mohammad NAH. Desalination: Conversion of Seawater to Freshwater. Kuala Lumpur; 2013.

[8] Heihsel M, Lenzen M, Malik A, Geschke A. The carbon footprint of desalination. Desalination 2019;454:71–81. https://doi.org/10.1016/j.desal.2018.12.008.

[9] Fu F, Wang Q. Removal of heavy metal ions from wastewaters: a review. J Environ Manage 2011;92:407–18. https://doi.org/10.1016/j.jenvman.2010.11.011.

[10] Semiat R. Present and Future. Water Int 2000;25:54–65. https://doi.org/10.1080/02508060008686797.

[11] El-Dessouky HT, Ettouney HM, Al-Roumi Y. Multi-stage flash desalination: present and future outlook. Chem Eng J 1999;73:173–90. https://doi.org/10.1016/s1385-8947(99)00035-2.

[12] Turek M, Mitko K, Piotrowski K, Dydo P, Laskowska E, Jakóbik-Kolon A. Prospects for high water recovery membrane desalination. Desalination 2017;401:180–9. https://doi.org/10.1016/j.desal.2016.07.047.

[13] Seo SD, Hong SY, Sum AK, Lee K-H, Lee JD, Lee BR. Thermodynamic and kinetic analysis of gas hydrates for desalination of saturated salinity water. Chem Eng J 2019;370:980–7. https://doi.org/10.1016/j.cej.2019.03.278.

[14] Başaran ST, Gökçekuş H, Orhon D, Sözen S. Autonomous desalination for improving resilience and sustainability of water management in North Cyprus. Desalination Water Treat 2020;177:283–9. https://doi.org/10.5004/dwt.2020.25090.

[15] Subramani A, Jacangelo JG. Emerging desalination technologies for water treatment: a critical review. Water Res 2015;75:164–87. https://doi.org/10.1016/j.watres.2015.02.032.

[16] Skuse C, Gallego-Schmid A, Azapagic A, Gorgojo P. Can emerging membrane-based desalination technologies replace reverse osmosis? Desalination 2021;500:114844. https://doi.org/10.1016/j.desal.2020.114844.

[17] Makogon Y. Hydrates of Hydrocarbons. Tulsa, OK: PennWell Books; 1997.

[18] Truong-Lam H, Kim S, Seo S, Jeon C-J, Lee JD. Water purifying by gas hydrate: potential applications to desalination and wastewater treatments. Chem Eng Trans 2020;78:67–72. https://doi.org/10.3303/CET2078012.

[19] Max, M. D. Hydrate Desalination or Water Purification. U.S. Patent 6,767,471B2, July 27, 2004.

[20] Babu P, Nambiar A, Chong ZR, Daraboina N, Albeirutty M, Bamaga OA, et al. Hydrate-based desalination (HyDesal) process employing a novel prototype design. Chem Eng Sci 2020;218:115563. https://doi.org/10.1016/j.ces.2020.115563.

[21] Koh CA, Sloan ED, Sum AK, Wu DT. Fundamentals and applications of gas hydrates. Annu Rev Chem Biomol Eng 2011;2:237–57. https://doi.org/10.1146/annurev-chembioeng-061010-114152.

[22] Park K-N, Hong SY, Lee JW, Kang KC, Lee YC, Ha M-G, et al. A new apparatus for seawater desalination by gas hydrate process and removal characteristics of dissolved minerals (Na+, Mg2+, Ca2+, K+, B3+). Desalination 2011;274:91–6. https://doi.org/10.1016/j.desal.2011.01.084.

[23] Dong H, Zhang L, Ling Z, Zhao J, Song Y. The controlling factors and ion exclusion mechanism of hydrate-based pollutant removal. ACS Sustain Chem Eng 2019;7:7932–40. https://doi.org/10.1021/acssuschemeng.9b00651.

[24] Youssef PG, AL-Dadah RK, Mahmoud SM. Comparative analysis of desalination technologies. Energy Procedia 2014;61:2604–7. https://doi.org/10.1016/j.egypro.2014.12.258.

[25] Fakharian H, Ganji H, Naderifar A. Desalination of high salinity produced water using natural gas hydrate. J Taiwan Inst Chem Eng 2017;72:157–62. https://doi.org/10.1016/j.jtice.2017.01.025.

[26] Alawad SM, Mansour RB, Al-Sulaiman FA, Rehman S. Renewable energy systems for water desalination applications: a comprehensive review. Energy Convers Manag 2023;286:117035. https://doi.org/10.1016/j.enconman.2023.117035.

[27] Sangwai JS, Patel RS, Mekala P, Mech D, Busch M. Desalination of seawater using gas hydrate technology-current status and future direction. In: In Proceedings of the 18th International Conference on Hydraulics. HYDRO: Water Resources, Coastal and Environmental Engineering; 2013. p. 434–40.

[28] Al-Qaraghouli A, Kazmerski LL. Comparisons of technical and economic performance of the main desalination processes with and without renewable energy Coupling. Natl Renew Energy Lab 2012:1–8.

[29] Curto D, Franzitta V, Guercio A. A review of the water desalination technologies. Appl Sci (basel) 2021;11:670. https://doi.org/10.3390/app11020670.

[30] Song Y, Dong H, Yang L, Yang M, Li Y, Ling Z, et al. Hydrate-based heavy metal separation from aqueous solution. Sci Rep 2016;6:21389. https://doi.org/10.1038/srep21389.

[31] Kang KC, Linga P, Park K-N, Choi S-J, Lee JD. Seawater desalination by gas hydrate process and removal characteristics of dissolved ions (Na+, K+, Mg2+, Ca2+, B3+, Cl−, SO42−). Desalination 2014;353:84–90. https://doi.org/10.1016/j.desal.2014.09.007.

[32] Corak D, Barth T, Høiland S, Skodvin T, Larsen R, Skjetne T. Effect of subcooling and amount of hydrate former on formation of cyclopentane hydrates in brine. Desalination 2011;278:268–74. https://doi.org/10.1016/j.desal.2011.05.035.

[33] Nallakukkala S, Lal B. Seawater and produced water treatment via gas hydrate: Review. J Environ Chem Eng 2021;9:105053. https://doi.org/10.1016/j.jece.2021.105053.

[34] Babu P, Kumar R, Linga P. Unusual behavior of propane as a co-guest during hydrate formation in silica sand: potential application to seawater desalination and carbon dioxide capture. Chem Eng Sci 2014;117:342–51. https://doi.org/10.1016/j.ces.2014.06.044.

[35] Linga P, Babu P, Nambiar AP (2018) A clathrate hydrate desalination method. WO/2018/156083.

[36] Zheng J-N, Yang M. Experimental investigation on novel desalination system via gas hydrate. Desalination 2020;478:114284. https://doi.org/10.1016/j.desal.2019.114284.

[37] Englezos P. Applications of Clathrate (Gas) Hydrates. Clathrate Hydrates 2022:749–81. https://doi.org/10.1002/9783527695058.ch16.

[38] Hečko D, Malcho M, Mičko P, Kantová NČ, Kolková Z, Hrabovský P, et al. Controlled production of natural gas hydrates in an experimental device with an internal circulation circuit. Appl Sci (basel) 2021;12:312. https://doi.org/10.3390/app12010312.

[39] Dendy Sloan E, Jr KCA. Clathrate hydrates of natural gases, third edition. 3rd ed. Boca Raton, FL: CRC Press; 2007.

[40] Taylor CE, editor. Advances in the Study of Gas Hydrates. New York, NY: Springer; 2014.

[41] Kumagai M, Endoh K. Effects of kinematic viscosity and surface tension on gas entrainment rate of an impinging liquid jet. J Chem Eng Japan 1982;15:427–33. https://doi.org/10.1252/jcej.15.427.

[42] Vysniauskas A, Bishnoi PR. A kinetic study of methane hydrate formation. Chem Eng Sci 1983;38:1061–72. https://doi.org/10.1016/0009-2509(83)80027-x.

[43] Englezos P, Kalogerakis N, Dholabhai PD, Bishnoi PR. Kinetics of formation of methane and ethane gas hydrates. Chem Eng Sci 1987;42:2647–58. https://doi.org/10.1016/0009-2509(87)87015-x.

[44] Happel J, Hnatow MA, Meyer H. The study of separation of nitrogen from methane by hydrate formation using a novel apparatusa. Ann N Y Acad Sci 1994;715:412–24. https://doi.org/10.1111/j.1749-6632.1994.tb38854.x.

[45] Nakajima Y, Takaoki T, Ohgaki K, Ot, S. Use of Hydrate Pellets for Transportation of Natural Gas-II-Proposition of Natural Gas Transportation in form of Hydrate Pellets. In Proceeding of the 4th International Conference on Gas Hydrates, Yokohama, Japan, May 19–23, 2002.

[46] Mork M, Gudmundsson JS. Hydrate formation rate in a continuous stirred tank reactor: experimental results and bubble-to-crystal model. In Proceeding of the 4th International Conference on Gas Hydrates, Yokohama, Japan, May 19–23, 2002.
[47] Pedchenko N, Zezekalo I, Pedchenko L, Pedchenko M. Research into phase transformations in reservoir systems models in the presence of thermodynamic hydrate formation inhibitors of high concentration. E3S Web Conf 2021;230:01014. https://doi.org/10.1051/e3sconf/202123001014.
[48] Pedchenko M, Pedchenko N, Pedchenko L. Reducing the man-made impact of hydrate formation inhibitors on the environment by applying gas hydrate technologies. IOP Conf Ser: Earth Environ Sci 2025;1491:012038. https://doi.org/10.1088/1755-1315/1491/1/012038.